Entwined dimer formation from self-complementary bis-acridiniums

Henri-Pierre Jacquot de Rouville, Nathalie Zorn, Emmanuelle Leize-Wagner, Valérie Heitz

Entwined dimer formation from self-complementary bis-acridiniums

Henri-Pierre Jacquot de Rouville, Nathalie Zorn, Emmanuelle Leize-Wagner, Valérie Heitz

Journal Name

COMMUNICATION

Entwined Dimers Formation from Self-Complementary Bis-Acridiniums

Received 00th January 20xx,
Accepted 00th January 20xx

DOI: 10.1039/x0xx00000x

www.rsc.org/

Henri-Pierre Jacquot de Rouville,*[a,b] Nathalie Zorn,[c] Emmanuelle Leize-Wagner,[c] and Valérie Heitz*[b]

A dicationic tweezer incorporating two acridinium moieties linked by a 2,6-diphenylpyridine spacer was shown to self-assemble in an entwined dimer both in acetonitrile and water. The reaction was studied according to solvent polarity, temperature and concentration conditions. The entwined structure was confirmed in the solid state by single-crystal X-ray diffraction.

Molecular recognition and self-assembly are essential phenomena[1] governing the formation of complex assemblies in living organisms (such as the lipid bilayer of cell membranes, the double helical structure of DNA, G-quadruplex secondary structures, etc.). Such high structural organisation relies on the combination and cooperation of multiple weak interactions (hydrophobic interactions, hydrogen-bonding, van der Waals forces, π-π interactions) and strongly depend on the information hold in the molecular structure of the individual components (shape and functional groups).

Self-assembling systems of identical units can be considered as the simplest process for the elaboration of larger and more useful discrete assemblies in a reliable manner.[2] Over the last decades, hydrogen-bonded,[3] metal-templated[4] and hydrophobic[5] driven one-component self-assemblies have been designed, synthesized and characterized in solution. However, few examples involving the self-association in solution of the same discrete subunits by π-π stacking interactions have been reported.[6] Among these systems, [*c2*]daisy-chain can be cited as a class of self-associated dimers.[7] They are based on π–donor-π–acceptor recognition subunits between a macrocyclic moiety and a complementary acyclic station. More recently, π-dimerization of reduced methylviologen was exploited to self-associate oligoviologens as the result of radical-radical interactions.[8]

An alternative approach relies on tweezer-shaped systems[9] which are non-cyclic molecular systems pre-organizing a minimum of two recognition units linked by a spacer acting as a complementary recognition unit. This strategy has been used by Haino *et al.* who described a bis-porphyrin dimer where both porphyrins interact with the electro-deficient pyridine component of the spacer of an identical molecule.[10]

Systems incorporating two acridinium units have mostly been used as receptor for the recognition of electron rich aromatic guest molecules.[11] In the present work, we report i) the synthesis of a new bis-acridinium tweezer, ii) the characterization of its self-association into an entwined dimer in solution (organic and aqueous media) and iii) its solid-state characterization.

Inspired by Laursen *et al.*,[12] a new convergent synthetic route was undertaken for the synthesis of the targeted tweezer **1•2PF$_6$** (Scheme 1). First, metal-halogen exchange of 1,3-dibromobenzene (1 eq.) using *n*-BuLi (1 eq.) in hexanes (2.5 mol·L^{-1}), then followed by addition of 10-methyl-9(10H)-acridone[13] at –78°C (1 eq.) led to the corresponding hydroxy-acridane intermediate. Acidification of a solution of the hydroxy-acridane intermediate with HCl (37 wt. %), followed by anion metathesis using KPF_6, led to **2•PF$_6$** as a yellowish precipitate in 85% yield. Since the cationic product of the Miyaura borylation cross-coupling reaction of **2•PF$_6$** turned out to be difficult to isolate, dearomatization of the **2•PF$_6$** was thus performed using $NaBH_4$ (90 wt. %, 10 eq.) in CH_3OH. After column chromatography, the hydro-acridane **3** was isolated in 72% yield. Compound **3** was then reacted with bis(pinacolato)diboron (1.1 eq) under Miyaura conditions using $Pd(dppf)Cl_2$ (10%) as catalyst and KOAc as base (3 eq.) in DMF. The corresponding boronic ester **4** was obtained in 76% yield. The di-functionalization of 2,6-dibromopyridine with **4** (2.1 eq.) in a C_{sp2}-C_{sp2} palladium-catalysed coupling was achieved using

[a] Univ Paris Diderot, Sorbonne Paris Cite, ITODYS, UMR CNRS 7086, rue J-A de Baif, 75013 Paris, France. E-mail: h-p.jacquot@univ-paris-diderot.fr
[b] Laboratoire de Synthèse des Assemblages Moléculaires Multifonctionnels, Institut de Chimie de Strasbourg, CNRS/UMR 7177, 4, rue Blaise Pascal, 67000 Strasbourg, France. E-mail: v.heitz@unistra.fr, hpjacquot@unistra.fr
[c] Laboratoire de Spectrométrie de Masse des Interactions et des Systèmes (LSMIS), UMR 7140 (Unistra-CNRS), Université de Strasbourg, France
† Footnotes relating to the title and/or authors should appear here.
Electronic Supplementary Information (ESI) available: [details of any supplementary information available should be included here]. See DOI: 10.1039/x0xx00000x

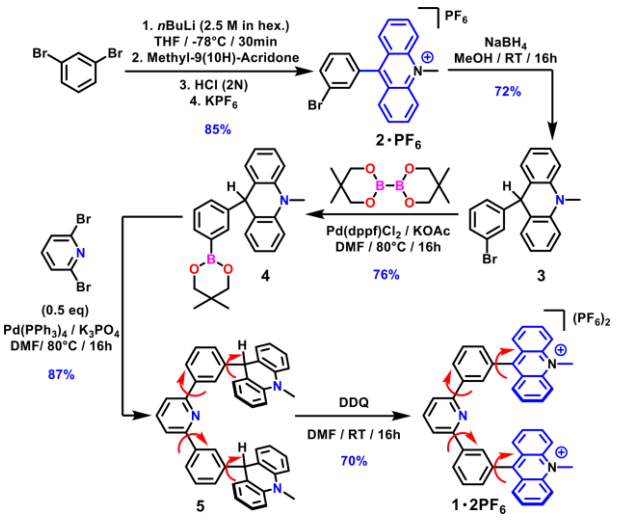

Scheme 1 Synthesis of **1·2PF$_6$** from 1,3-dibromobenzene as starting material.

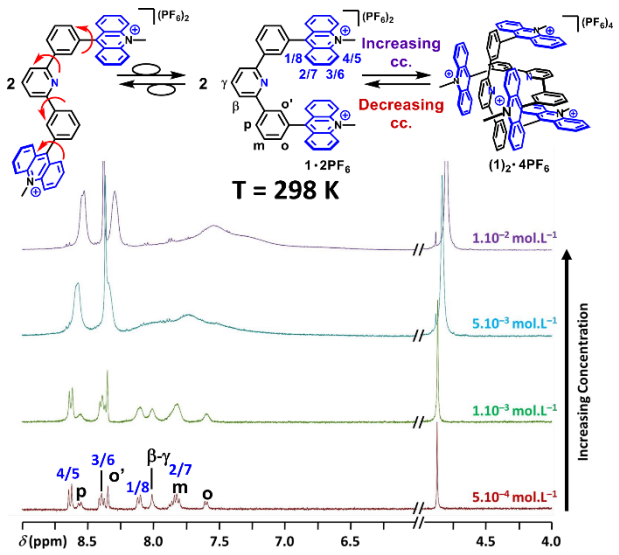

Fig. 1 ^{1}H NMR (500 MHz, CD_3CN, 298 K) spectra of **1·2PF$_6$** at $1{\cdot}10^{-2}$, $5{\cdot}10^{-3}$, $1{\cdot}10^{-3}$ and $5{\cdot}10^{-4}$ mol·L^{-1}.

$Pd(PPh_3)_4$ (20%) and K_3PO_4 (3 eq.) as base in DMF. After purification, the bis-acridane **5** was isolated in 87% yield. Oxidation of **5** was performed using 2,6-dichloro-5,6-dicyano-1,4-quinone (DDQ) in DMF and the crude mixture was poured into an aqueous solution of KPF_6. The yellow precipitate of **1·2PF$_6$** was filtered off, washed with H_2O and isolated in 70 % yield.

The ^{1}H NMR spectrum (CD_3CN, c = $1{\cdot}10^{-2}$ mol·L^{-1}, 298 K) of **1•2PF$_6$** showed time-averaged signals resulting from a slow exchange regime. Initially, this observation was attributed to conformational exchange processes in **1•2PF$_6$** but this hypothesis was excluded by variable concentration experiments (Figure 1). At a concentration of $5{\cdot}10^{-4}$ mol·L^{-1} (T = 298 K), the ^{1}H NMR signals became narrow and the assignments of all protons were in accordance with the monomeric species. Remarkably, this spectrum exhibits similar chemical shifts than our previously reported Triphenyl-bis-acridinium receptor which was in a fast exchange regime at $5{\cdot}10^{-4}$ mol·L^{-1}.[13] More especially, the chemical shifts of the acridinium protons (δ(H$_{1/8}$) = 8.13, δ(H$_{2/7}$) = 7.86, δ(H$_{3/6}$) = 8.41 and δ(H$_{4/5}$) = 8.64 ppm) are similar for both molecules (see ESI, Figures S3.43-3.44). This observation suggests that the acridinium protons are not affected by the difference in the electronic environment of the spacer and experienced a solvated environment close to the isolated monomer of **1•2PF$_6$**. As a consequence, this concentration-dependant behaviour was best interpreted in terms of a dynamic equilibrium between oligomeric species in solution, more especially between the monomer **1•2PF$_6$** and its dimer **(1)$_2$•4PF$_6$**.

Mass spectrometry analysis (ESI-TOF) gave also some evidence on the presence of the dimer in the gas phase. Injection of a solution of **1•2PF$_6$** in CH_3CN (c = $1{\cdot}10^{-3}$ mol·L^{-1}) led to peaks at m/z at 760.23, 1665.42, 2571.62 and 3477.81 corresponding to the loss of a PF_6^- counter-ion for the monomer **[1•PF$_6$]$^+$** and the dimeric **[1$_2$•3PF$_6$]$^+$**, trimeric **[1$_3$•5PF$_6$]$^+$** and tetrameric **[1$_4$•7PF$_6$]$^+$** aggregates respectively (see SI, Figure S3.45). Upon dilution (c = $1{\cdot}10^{-4}$ and $1{\cdot}10^{-5}$ mol·L^{-1}), the signal corresponding to the dimer aggregate was monitored continuously while those of **[1$_3$•5PF$_6$]$^+$** and **[1$_4$•7PF$_6$]$^+$** disappeared. The persistence of the **[1$_2$•3PF$_6$]$^+$** signal suggests that the dimer is a specific aggregate whereas the trimer and tetramer are non-specific aggregates.

Further insights into the dynamic equilibrium were given by ^{1}H NMR variable temperature experiments. Upon heating at 343 K, the spectrum characteristic of the monomer was observed at all concentrations (see ESI, Figure S3.34). However, recording spectrum at low temperature (T = 248 K) at a concentration of $1{\cdot}10^{-2}$ mol·L^{-1} showed evidence of the formation of a new discrete species (Figure 2). The spectrum shows sharp signals upfield-shifted in comparison to the monomer (e.g. $\Delta\delta$(H$_{1/8}$) = 1.01, $\Delta\delta$(H$_{2/7}$) = 0.50, $\Delta\delta$(H$_{3/6}$) = 0.19, $\Delta\delta$(H$_{4/5}$) = 0.19 ppm for the acridinium protons). Pronounced upfield shifts were also observed for the β and γ protons of the central pyridine ($\Delta\delta$(β) = 1.52 ppm and $\Delta\delta$(γ) = 0.68 ppm) thus witnessing π–π interactions between all aromatic moieties of the molecule.[14] This spectrum can be best interpreted as the result of a dimer of D_{2d} symmetry formed from two **1•2PF$_6$** molecules. The presence of the dimer **(1)$_2$•4PF$_6$** as a unique species (CD_3CN, c = $1{\cdot}10^{-2}$ mol·L^{-1}, 248 K) was also supported by DOSY experiments (see ESI, Figures 3.38-3.40) since all NMR signals were assigned to a unique diffusing species. The calculated hydrodynamic radius (R_H) was found to be 7.3 Å (corresponding to a diffusion coefficient (D) of 240 µm^2·s^{-1}) which is larger than the hydrodynamic radius of the **1.2PF$_6$** monomer (R_H = 6.6 Å; D = 297 µm^2·s^{-1} within the experimental error of ±5%). Upon dilution at 238 K, signals corresponding to the dimer and the monomer were simultaneously monitored in agreement with *Le Chatelier's principle*. At a concentration of $5{\cdot}10^{-4}$ mol·L^{-1}, the dimer-monomer ratio was found to be 7:3 corresponding to an estimated binding constant (K_a) of $7{\cdot}10^3$ L·mol^{-1} at 248 K.[15]

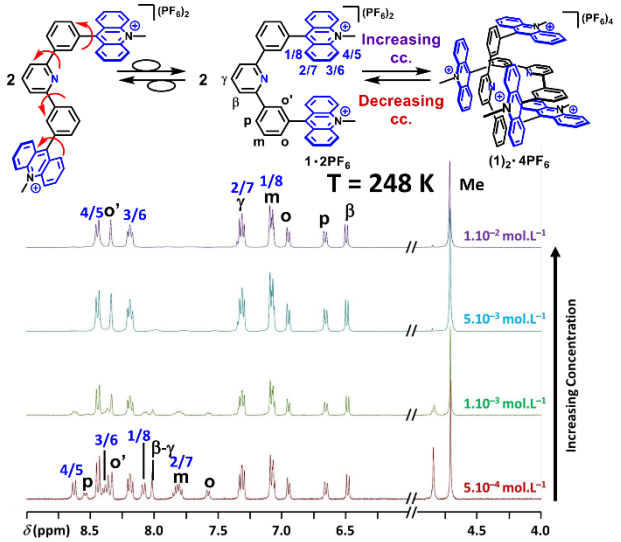

Fig. 2 ^{1}H NMR (500 MHz, CD_3CN, 248 K) spectra of **1·2PF$_6$** at $1{\cdot}10^{-2}$, $5{\cdot}10^{-3}$, $1{\cdot}10^{-3}$ and $5{\cdot}10^{-4}$ mol·L^{-1}. At 1.10^{-2} mol·L^{-1}, the assignments correspond to the protons of the dimer **(1)$_2$·4PF$_6$**. At 5.10^{-4} mol·L^{-1}, the dimer-monomer ratio is 7:3 and only the assignments of the protons of the monomeric species is shown.

The existence of this equilibrium was also confirmed by varying the solvent polarity of the medium. Equimolar solutions of **1·2PF$_6$** (c = $3{\cdot}10^{-3}$ mol·L^{-1}) were monitored at 298 K with an increasing percentage of DMSO-d^6 in CD_3CN (from 0% to 100%, see ESI, Figure S3.42). Upon increasing the polarity of the medium, the initial broad spectrum recorded in CD_3CN led to a well-resolved spectrum in pure DMSO-d^6 of the monomer. As expected, DMSO competes strongly with the π-interactions that stabilise the dimer. Therefore, the equilibrium between the dimer and the monomer is shifted towards to the monomer.

Single crystals suitable for X-ray diffraction were obtained from vapour diffusion of Et_2O into a CH_3CN solution of **1·2PF$_6$**.[16] The solid state structure exhibits the dimer that consists of two independent **1·2PF$_6$** molecules that entwined one another (Figure 3a-c). Both molecules adopt a U-shaped conformation (Figure 3d-f) where the two acridinium moieties of each **1·2PF$_6$** molecule are in a quasi-parallel arrangement ($d_{C9\text{-}C9}$ distances of 7.138(7) Å & 7.209(6) Å and $d_{N\text{-}N}$ distances of 7.180(7) Å & 7.064(5) Å leading to an averaged offset dihedral angle of 8.6°). The optimum distance between both acridinium moieties allows π-π stacking interactions with the 2,6-diphenylpyridine spacer of the second monomer of **(1)$_2$·4PF$_6$**. The 2,6-diphenylpyridine spacer exhibits a quasi-planar geometry (τ = 12.22° & 8.95°) thus facilitating its inclusion in between both acridinium subunits. Noteworthy, the nitrogen atoms of the central pyridines are aligned on the straight line formed by the two C9 atoms of the two interacting acridinium moieties. Noteworthy, the averaged methyl-methyl distance between the two entwined monomers ($d_{Me\text{-}Me}$ = 12.97 Å) is in good agreement with twice the estimated hydrodynamic radius obtained from the DOSY ($2R_H$ = 14.6 Å) thus giving further evidence of the presence of dimeric form in solution.

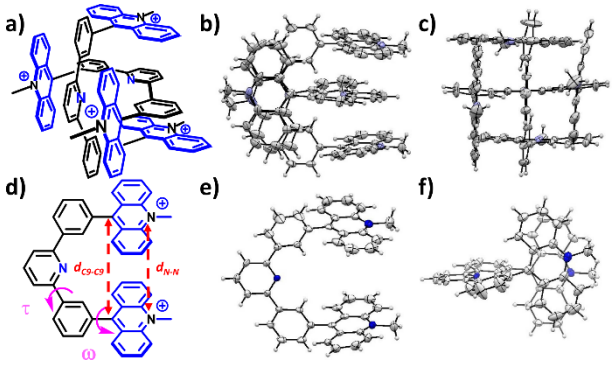

Fig. 3 Crystal structure views b-c and e-f of **(1)$_2$·4PF$_6$**. a) Scheme of the entwined dimer of **1·2PF$_6$**. b) Side view of the entwined dimer of **1·2PF$_6$** showing the π-π stacking between the acridinium moieties and the 2,6-diphenylpyridine spacer. c) Rear view of the entwined dimer. d) Scheme of a **1·2PF$_6$** monomer of **(1)$_2$·4PF$_6$**. e) Side view of a **1·2PF$_6$** monomer of **(1)$_2$·4PF$_6$** showing the U-shaped conformation. f) Top view of a **1·2PF$_6$** monomer of **(1)$_2$·4PF$_6$**.

We envisioned that hydrophobic interactions should favour the dimerization process of this aromatic compound. Therefore, **1·2PF$_6$** was converted to its corresponding chloride salts **1·2Cl** using tetrabutylammonium chloride (TBACl). The water soluble **1·2Cl** showed a well-resolved spectrum in D_2O at 298 K characteristic of a discrete species. The ^{1}H NMR spectrum at room temperature was analogous to the spectrum obtained at a concentration of $1{\cdot}10^{-2}$ mol·L^{-1} in CD_3CN at 248 K. More especially, the chemical shifts of the β protons of the central pyridine core (δ(H$_\beta$) = 6.65 ppm), the H$_o$ and H$_p$ protons of the outer phenyl groups (δ(H$_o$) = 7.01 ppm and δ(H$_p$) = 6.80 ppm) exhibit similar upfield shifts as observed for the dimer **(1)$_2$·4PF$_6$** in CD_3CN.[17] The presence of the dimer **(1)$_2$·4Cl** was confirmed by ^{1}H-^{1}H NOESY experiments (Figure 4). Through-space correlations between the pyridine protons and the methyl protons of the acridinium moieties suggests a close proximity of these two subunits as seen in the solid state structure. The central 2,6-diphenylpyridine spacer experienced the cone of anisotropy of the acridinium moieties (and reciprocally) thus explaining the chemical shifts observed in the ^{1}H NMR spectrum. These results show the monomer-dimer equilibrium is totally shifted to the dimeric form which enables each of the hydrophobic central pyridines to be shielded from the aqueous environment by two large π-cationic acridinium moieties. In other words, hydrophobic interactions reinforce the formation of the supramolecular dimer. Noteworthy, the same sharp ^{1}H NMR signals is observed in a concentration range from 10^{-2} to $5{\cdot}10^{-4}$ mol·L^{-1} in aqueous media corresponding to a K_a above $1{\cdot}10^5$ L·mol^{-1} at 298 K. Further evidence of the dimer formation were given by DOSY experiments (see ESI, Figure S3.41). The hydrodynamic radius was found to be in the same order of magnitude in D_2O (R_H = 7.3 Å; D = 263 µm²·s^{-1}) than in CD_3CN (R_H =7.3 Å; D = 240 µm²·s^{-1}) thus supporting a dimeric self-association in D_2O.

In conclusion, the synthesis of a molecular tweezer bearing two acridinium units connected to a 2,6-diphenylpyridine spacer was achieved in good yield according to a convergent synthetic

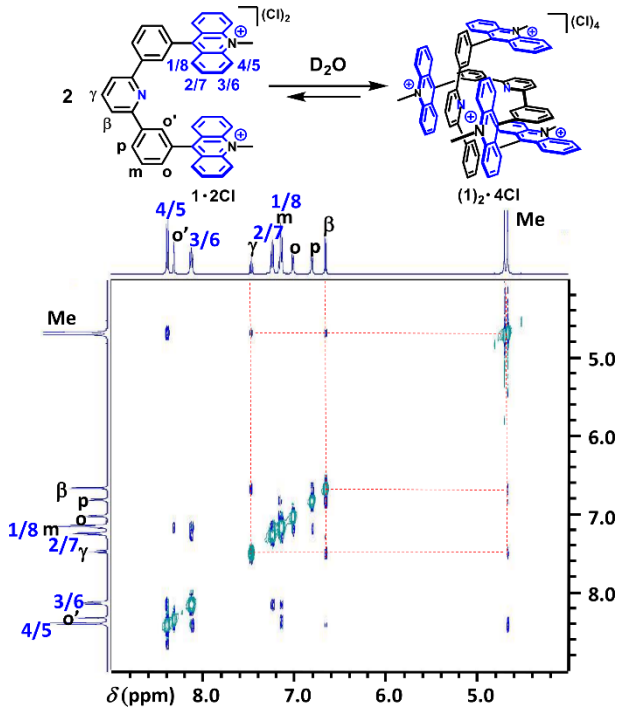

Fig. 4 ^{1}H-^{1}H NOESY (500 MHz, D_2O, 298 K, c = 5·10^{-3} mol·L^{-1}) spectrum of **(1)$_2$·4Cl**. Correlations between the β and γ protons of the pyridine with the methyl protons.

strategy. The tweezer shows an entwined dimeric structure in the solid-state resulting from π–π stacking interactions between the acridiniums units and the 2,6-diphenylpyridine spacer. In solution, the existing equilibrium between the monomeric and the dimeric forms of the molecule was evidenced in organic medium, with K_a = 7·10^3 L·mol^{-1} at in CD_3CN at 248 K. This equilibrium was shifted to the monomer upon increasing solvent polarity (DMSO-d^6), temperature and dilution (CD_3CN). In water, hydrophobic interactions lead to a complete shift of the equilibrium towards the dimer as demonstrated by NMR experiments. Work is now underway to design and synthesize functionalized bis-acridinium tweezers to explore their properties as supramolecular receptors.

This work was supported by the CNRS, the University Paris Diderot, and the University of Strasbourg. We are grateful to Dr. Corinne Bailly (Crystallographic Service) and to Dr. Bruno Vincent (NMR Service) of the Faculté de Chimie de l'Université.

Conflicts of interest

There are no conflicts to declare.

Notes and references

1 (a) D. J. Cram, J. M. Cram, *Science*, 1974, **183**, 803 – 809; (b) J.-M. Lehn, Science, 1985, **227**, 849–856; (c) J.-M. Lehn, Angew. Chem., 1990, **102**, 1347–1362; *Angew. Chem., Int. Ed. Engl.*, 1990, **29**, 1304–1319; (d) J.-M. Lehn, *Supramolecular Chemistry: Concepts and Perspectives*, Wiley-VCH, New York, NY, 1995; (e) J. Rebek Jr., *Chem. Soc. Rev.*, 1996, **25**, 255–264; (f) J. M. Spruell, *Pure Appl. Chem.*, 2010, **82**, 2281–2294.

2 M. M. Conn and J. Rebek Jr., *Chem. Rev.*, 1997, **97**, 1647–1668.

3 (a) M. R. Ghadiri, K. Kobayashi, J. R. Granja, R. K. Chadha and D. E. McRee, *Angew. Chem., Int. Ed. Engl.*, 1995, **34**, 93–95; (b) S.C. Zimmerman, F. Zeng, D. E. C. Reichert and S. V. Kolotuchin, *Science*, 1996, **271**, 1095–1098; (c) O. Mogck, V. Böhmer and W. Vogt, *Tetrahedron*, 1996, **52**, 8489–8496; (d) J. Kang and J. Rebek Jr., *Nature*, 1996, **382**, 239–241.

4 (a) C. Dietrich-Buchecker and J.-P. Sauvage, *Tetrahedron*, 1990, **46**, 503–512; (b) B. Hasenknopf, J.-M. Lehn, N. Boumediene, A. Dupont-Gervais, A. Van Dorsselaer, B. Kneisel and D. Fenske, *J. Am. Chem. Soc.*, 1997, **119**, 10956–10962; (c) D. A. Leigh, P. J. Lusby, S. J. Teat, A. J. Wilson and J. K. Y. Wong, *Angew. Chem., Int. Ed.*, 2001, **40**, 1538–1543; (d) J. J. Danon, A. Krüger, D. A. Leigh, J.-F. Lemonnier, A. J. Stephens, I. J. Vitorica-Yrezabal and S. L. Woltering, *Science*, 2017, **355**, 159–162.

5 (a) A. Muñoz de la Peña, T. T. Ndou, J. B. Zung, K. L. Greene, D. H. Live and I. M. Warner, *J. Am. Chem. Soc.*, 1991, **113**, 1572–1577; (b) F. Venema, A. E. Rowan and R. J. M. Nolte, *J. Am. Chem. Soc.*, 1996, **118**, 257–258.

6 (a) S. J. Holder, J. A. A. W. Elemans, J. J. J. M. Donners, M. J. Boerakker, R. de Gelder, J. Barberá, A. E. Rowan and R. J. M. Nolte, *J. Org. Chem.*, 2001, **66**, 391-399; (b) S. Ghosh, A. Wu, J. C. Fettinger, P. Y. Zavalij and L. Isaacs, *J. Org. Chem.*, 2008, **73**, 5915–5925.

7 (a) P. R. Ashton, I. Baxter, S. J. Cantrill, M. C. T. Fyfe, P. T. Glink, J. F. Stoddart, A. J. P. White and D. J. Williams, *Angew. Chem., Int. Ed.*, 1998, **37**, 1294–1297; (b) J. Rotzler and M. Mayor, *Chem. Soc. Rev.*, 2013, **42**, 44–62.

8 Y. Wang, M. Frasconi, W.-G. Liu, Z. Liu, A. A. Sarjeant, M. S. Nassar, Y. Y. Botros, W. A. Goddard III and J. F. Stoddart, *J. Am. Chem. Soc.*, 2015, **137**, 876−885.

9 (a) C.-W. Chen and H. W. Whitlock Jr., *J. Am. Chem. Soc.*, 1978, **100**, 4921–4922; (b) F.-G. Klärner and B. Kahlert, *Acc. Chem. Res.*, 2003, **36**, 919–932; (c) M. Linke-Schaetzel, C. E. Anson, A. K. Powell, G. Buth, E. Palomares, J. D. Durrant, T. S. Balaban and J.-M. Lehn, *Chem. Eur. J.*, 2006, **12**, 1931–1940; (d) M. Hardouin-Lerouge, P. Hudhomme and M. Sallé, *Chem. Soc. Rev.*, 2011, **40**, 30–43; (e) J. Leblond and A. Petitjean, *ChemPhysChem*, 2011, **12**, 1043–1051.

10 (a) T. Haino, T. Fujii and Y. Fukazawa, *Tetrahedron Lett.*, 2005, **46**, 257–260; (b) T. Haino, T. Fujii, A. Watanabe and U. Takayanagi, *Proc. Natl. Acad. Sci. USA*, 2009, **106**, 10477–10481.

11 (a) S. Claude, J.-M. Lehn, F. Schmidt and J.-P. Vigneron, *J. Chem. Soc., Chem. Commun.*, 1991, 1182–1185; (b) A. Petitjean, R. G. Khoury, N. Kyritsakas and J.-M. Lehn, *J. Am. Chem. Soc.*, 2004, **126**, 6637–6647.

12 T. J. Sørensen, A. Ø. Madsen and B. W. Laursen, *Chem. Eur. J.*, 2014, **20**, 6391–6400.

13 A. Gosset, Z. Xu, F. Maurel, L.-M. Chamoreau, S. Nowak, G. Vives, C. Perruchot, V. Heitz and H.-P. Jacquot de Rouville, *New J. Chem.*, 2018, **42**, 4728–4734.

14 M. Fujita, F. Ibukuro, H. Hagihara and K. Ogura, *Nature*, 1994, **367**, 720–723.

15 UV-Vis spectra in acetonitrile did not show any charge transfer bands when compared to the spectra of the 2,6-diphenylpyridine and the 9-phenyl-N-acridinium moieties within the 250-780 nm spectral range (see ESI, Figures S4).

16 Crystal data for **1.2PF$_6$**: 2($C_{45}H_{33}N_3$),4(F_6P),C_2H_3N, orange prism, crystal size 0.36 x 0.34 x 0.28 mm^3, monoclinic, space group $P2_1/c$, a = 12.8107(4) Å, b = 27.4670(10) Å, c = 25.2827(10) Å, α = 90°, β = 113.746(2)°, γ = 90°, V = 8143.1(5) Å^3, Z = 4, ρ_{calc} = 1.511 , T = 173(2) K, $R_1(F^2 > 2\sigma F^2)$ = 0.0977, wR_2 = 0.2449. Out of 87028 reflections a total of 19650 were unique. CCDC–1856039

17 Noteworthy, no dilution effect (see ESI, Figure S3.37) or temperature effect (see ESI, Figure S3.46) are observed suggesting a stable dimeric assembly.